Synthesis and Characterization of Water-Soluble [Pd(triphosphine)(CH_3CN)](BF_4)$_2$ Complexes for CO_2 Reduction

Andrew M. Herring, Bryan D. Steffey, Alex Miedaner, Sheryl A. Wander, and Daniel L. DuBois*

National Renewable Energy Laboratory, 1617 Cole Boulevard, Golden, Colorado 80401

Received October 7, 1994[⊗]

The syntheses of the triphosphine ligands RP($CH_2CH_2PR'_2$)$_2$ (R = $CH_2CH_2CH_2OH$ and R′ = Et, HOPetpE; R = Ph and R′ = $CH_2CH_2P(O)(OEt)_2$, etpEPO; R = Me_2N and R′ = Et, MNetpE; R = *i*-Pr_2N and R′ = Et, IPNetpE; R = Ph and R′ = NMe_2, etpMN) are described. The reaction of [Pd(CH_3CN)$_4$](BF_4)$_2$ with these ligands forms [Pd(triphosphine)(CH_3CN)](BF_4)$_2$ complexes that are all water soluble with the exception of [Pd(IPNetpE)(CH_3CN)](BF_4)$_2$. The labile acetonitrile ligands are easily substituted by triethylphosphine to form [Pd(triphosphine)(PEt_3)](BF_4)$_2$ complexes. The triethylphosphine complexes undergo quasi-reversible two-electron reductions while the corresponding acetonitrile complexes undergo two, closely spaced, irreversible, one-electron reductions. [Pd(HOPetpE)(CH_3CN)](BF_4)$_2$ and [Pd(etpEPO)(CH_3CN)](BF_4)$_2$ are catalysts for the electrochemical reduction of CO_2 to CO in both dimethylformamide and buffered aqueous solutions. Kinetic studies are reported for [Pd(HOPetpE)(CH_3CN)](BF_4)$_2$ in dimethylformamide.

Introduction

There is currently considerable interest in the development of water-soluble organometallic complexes for catalytic applications. A number of excellent reviews and well-referenced papers have appeared on this subject.[1] The primary advantages of water-soluble catalysts are the ease of separation and recovery of the catalysts from an organic phase containing the substrate and the environmental benefits of using water to replace organic solvents. One well-known example of an industrial process that uses water-soluble catalysts is the hydroformylation of olefins.[2] Another application for which water-soluble catalysts may have significant advantages is for electrochemical processes in which the much lower resistance of aqueous solutions compared to that of organic solutions[3] would improve the energy efficiency of the process. Minimizing energy losses is of particular importance in processes designed to generate or use fuels.

The electrochemical reduction of carbon dioxide to carbon monoxide in acidic acetonitrile or dimethylformamide solutions is catalyzed by [Pd(triphosphine)(solvent)](BF_4)$_2$ complexes.[4] These complexes exhibit interesting catalytic properties, including high turnover rates, high selectivities under appropriate conditions, and relatively positive reduction potentials. However, these complexes are not soluble in water. In this paper, we describe the preparation and characterization of water-soluble analogues of these complexes. Of particular interest is the effect of an aqueous environment on the rates and selectivities of these catalysts. Previous research with rhodium-based hydrogenation catalysts has shown both beneficial and detrimental effects on catalyst selectivity.[2,5] The water-soluble [Pd(HOPetpE)(CH_3CN)](BF_4)$_2$ and [Pd(etpEPO)(CH_3CN)](BF_4)$_2$ complexes described in this paper exhibit slightly reduced selectivities for CO production in aqueous solutions compared to those of acidic dimethylformamide solutions.

Results

Synthesis and Characterization of Ligands and Complexes. In principle, linear triphosphine ligands can be modified with polar water-soluble functional groups on either the terminal phosphorus atoms, the central phosphorus atom, or the ethylene bridges linking the three phosphorus atoms. This paper deals with the first two approaches. Modification of the central phosphorus atom of the triphosphine ligand can be achieved using the synthetic sequence shown in Scheme 1. The free-radical-catalyzed addition of diethylphosphine to divinyl(diisopropylamino)phosphine produces the triphosphine ligand **1**. The ^{31}P NMR spectrum of this compound consists of a doublet and a triplet for the terminal and central phosphorus atoms, respectively. The magnitude of the coupling constants and the chemical shift values are within the range expected for a triphosphine ligand with ethylene bridges.[6,7] The ^1H NMR spectrum is also consistent with the proposed structure (see Experimental Section). Hydrolysis of **1** gives the secondary phosphine oxide **2**. Compound **2** exhibits a large P−H coupling (447 Hz) in both the ^1H NMR and proton-coupled ^{31}P NMR spectra, which is consistent with a proton bound directly to a pentavalent phosphorus atom.[8] The chemical shifts observed

[⊗] Abstract published in *Advance ACS Abstracts,* February 1, 1995.

(1) Barton, M.; Atwood, J. D. *J. Coord. Chem.* **1991**, *24*, 43−67. Ellis, J. W.; Harrison, K. N.; Hoye, P. A. T.; Orpen, A. G.; Pringle, P. G.; Smith, M. B. *Inorg. Chem.* **1992**, *31*, 3026−3033. Darensbourg, D. J.; Joo, F.; Kannisto, M.; Katho, A.; Reibenspies, J. H.; Daigle, D. J. *Inorg. Chem.* **1994**, *33*, 200−208. Avey, A.; Schut, D. M.; Weakley, T. J. R.; Tyler, D. R. *Inorg. Chem.* **1993**, *32*, 233−236. Bartik, T.; Bunn, B. B.; Bartik, B.; Hanson, B. E. *Inorg. Chem.* **1994**, *33*, 164−169.

(2) Kuntz, E. G. *CHEMTECH* **1987**, 570−575.

(3) Sawyer, D. T.; Roberts, J. L., Jr. *Experimental Electrochemistry for Chemists*; Wiley: New York, 1974; pp 188, 226.

(4) DuBois, D. L.; Miedaner, A.; Haltiwanger, R. C. *J. Am. Chem. Soc.* **1991**, *113*, 8753−8764.

(5) Amrani, Y.; Lecomte, L.; Sinou, D.; Bakos, J.; Toth, I.; Heil, B. *Organometallics* **1989**, *8*, 542−547 and references therein.

(6) King, R. B. In *Catalytic Aspects of Metal Phosphine Complexes*; Alyea, E. C., Meek, D. W., Eds.; Advances in Chemistry Series 196; American Chemical Society: Washington, DC, 1982; pp 313−323.

(7) DuBois, D. L.; Myers, W. H.; Meek, D. W. *J. Chem. Soc., Dalton Trans.* **1975**, 1011−1015.

0020-1669/95/1334-1100$09.00/0

Scheme 1

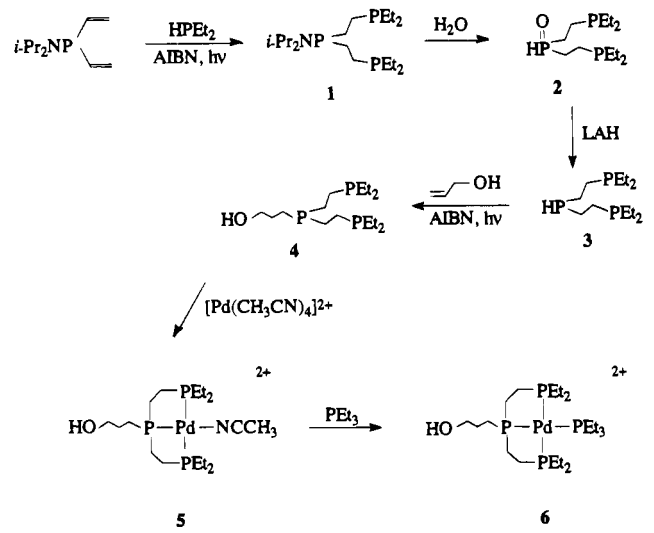

for the central and terminal phosphorus atoms (see Table 1) are also in the range expected for a secondary phosphine oxide and tertiary phosphines.[9] Reduction of **2** with lithium aluminum hydride (LAH) results in triphosphine ligand **3**, for which the central phosphorus atom is a secondary phosphine. This compound is an air-sensitive liquid that distills at reduced pressure without decomposition. A P−H coupling is observed for compound **3** in both ^{1}H NMR and proton-coupled ^{31}P NMR spectra. The magnitude of this coupling (193 Hz) is appropriate for a trivalent phosphorus atom.[8] The chemical shifts of the triplet and doublet observed in the ^{31}P NMR spectrum (see Table 1) closely match the values calculated (−19 and −54 ppm, respectively) using standard equations and substituent parameters.[4,9] Free-radical addition of the P−H bond of **3** to allyl alcohol forms ligand **4** (HOPetpE), which contains a 3-hydroxypropyl substituent on the central phosphorus atom. The doublet and triplet observed in the ^{31}P NMR spectrum of **4** are expected for a symmetrical, linear triphosphine ligand, and the calculated (−19 and −22 ppm, respectively) and observed chemical shifts shown in Table 1 support the proposed substituents. ^{1}H NMR and infrared spectra confirm the presence of OH and OCH_2 functional groups of a hydroxypropyl substituent (see the Experimental Section). Reaction of **4** with $[Pd(CH_3CN)_4](BF_4)_2$ produces $[Pd(HOPetpE)(CH_3CN)](BF_4)_2$, **5**, a yellow hygroscopic solid. The ^{31}P NMR spectrum of **5** is a doublet and a triplet with chemical shifts and a coupling constant typical of this class of compounds.[4,10] A methyl resonance at 2.08 ppm in the ^{1}H NMR spectrum recorded in acetone-d_6 indicates the presence of acetonitrile. Two bands at 2298 and 2326 cm^{-1} in the infrared spectrum of a Nujol mull of **5** are assigned to coordinated acetonitrile.[11] Substitution of the acetonitrile ligand of **5** with triethylphosphine produces **6**. The two doublets of triplets in the ^{31}P NMR spectrum of **6** are assigned to triethylphosphine and the central phosphorus atom, P_C, of the triphosphine ligand. The doublet splitting arises from the strong trans P−P coupling between triethylphosphine and P_C, and the triplet splitting is caused by cis coupling of these two phosphorus nuclei to the terminal phosphorus atoms, P_T, of the triphosphine ligand. A doublet of doublets is observed for the terminal phosphorus atoms.

The preparation of the triphosphine ligand **7**, etpEPO, has been described previously.[12] The terminal tertiary phosphorus atoms of this triphosphine ligand are modified with polar diethyl phosphonate groups. Modification of monodentate ligands with this functional group using a slightly different synthetic approach produced water-soluble monodentate phosphine ligands.[13] Reaction of etpEPO with $[Pd(CH_3CN)_4](BF_4)_2$ forms $[Pd(etpEPO)(CH_3CN)](BF_4)_2$, **8**, as shown in eq 1. This complex is

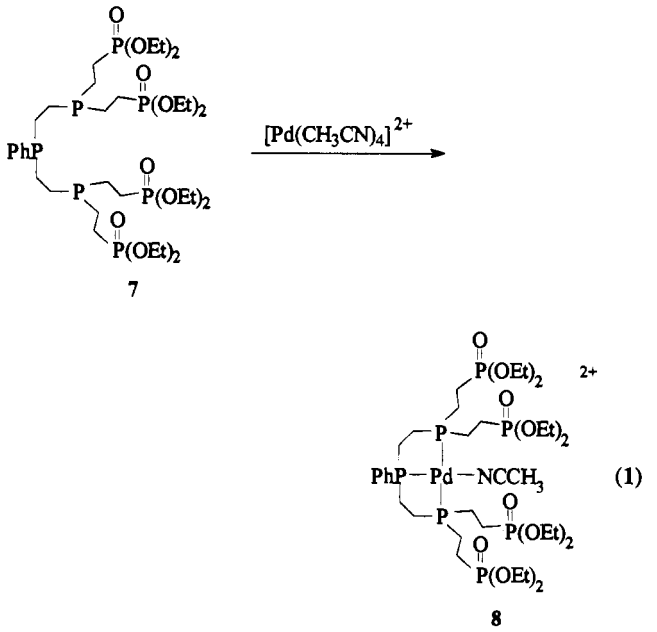

extremely hygroscopic and quite water soluble. The ^{31}P NMR spectrum of **8** consists of three groups of resonances as shown by the bottom trace in Figure 1. The resonance assigned to the central phosphorus atom of the triphosphine ligand is a simple triplet at approximately 118 ppm. The resonances for the terminal tertiary phosphine atoms (~61 ppm) and the phosphonate phosphorus atoms (~30 ppm) are more complex. A simulation of this spectrum using the parameters listed in Table 1 is shown by the trace at the top of Figure 1. The terminal phosphonate groups of the triphosphine ligand occupy two slightly different environments. The phosphonate substituents and the phenyl group of the central phosphorus atom can be on the same or opposite sides of the square plane defined by palladium and its coordination sphere. This accounts for the two different chemical shifts observed for the phosphonate phosphorus atoms. The presence of a coordinated acetonitrile ligand is indicated by the presence of bands at 2312 and 2349 cm^{-1} in the infrared spectrum of $[Pd(etpEPO)(CH_3CN)](BF_4)_2$ in dichloromethane. The labile acetonitrile ligand is readily displaced with triethylphosphine, trimethyl phosphite, or tris(hydroxymethyl)phosphine to form the square planar complexes $[Pd(etpEPO)PEt_3](BF_4)_2$, $[Pd(etpEPO)P(OCH_3)_3](BF_4)_2$, $[Pd(etpEPO)P(CH_2OH)_3](BF_4)_2$, **9a−c**. In the case of triphenylphosphine, however, the reaction does not go to completion. Addition of a 15% excess of triphenylphosphine to a solution of $[Pd(etpEPO)(CH_3CN)](BF_4)_2$ in acetonitrile produces approximately 60% of the triphenylphosphine adduct, $[Pd(etpEPO)PPh_3](BF_4)_2$, **9d**, after 4 days. Presumably this is a result of

(8) Smith, D. J. H. In *Comprehensive Organic Chemistry Vol. 2, Nitrogen Compounds, Carboxylic Acids, Phosphorus Compounds*; Barton, D., Ollis, W. D., Eds.; Pergamon: New York, 1979; p 1125.
(9) Tebby, J. C. In *Phosphorus-31 NMR Spectroscopy in Stereochemical Analysis, Organic Compounds and Metal Complexes;* Verkade, J. G., Quin, L. D., Eds.; Methods in Stereochemical Analysis Series No. 8; VCH: Deerfield Beech, FL, 1987; p 36. Fluck, E.; Heckmann, G. *Ibid.*, pp 88−93.
(10) DuBois, D. L.; Miedaner, A. *J. Am. Chem. Soc.* **1987**, *109*, 113−117.
(11) Storhoff, B. N.; Lewis, H. C., Jr. *Coord. Chem. Rev.* **1977**, *23*, 1−29.
(12) Miedaner, A.; Curtis, C. J.; DuBois, D. L. *Inorg. Chem.* **1994**, *33*, 5482−5490.
(13) Ganguly, S.; Mague, J. T.; Roundhill, D. M. *Inorg. Chem.* **1992**, *31*, 3500−3501.

Table 1. ^{31}P NMR Data for Ligands and Complexes

compound	$\delta(P_T)$,[a] ppm	$\delta(P_C)$,[a] ppm	$\delta(P_L)$,[a] ppm	$\delta(P_A)$,[a] ppm	^2J(TC), Hz	^2J(LC), Hz	^2J(LT), Hz	^2J(AT), Hz
H(O)etpE, **2**	−17.3	56.1			23.8			
HetpE, **3**	−18.6	−55.9			20.9			
HOPetpE, **4**	−17.8	−21.5			19.1			
[Pd(HOPetpE)(CH_3CN)](BF_4)$_2$, **5**	63.7	115.3			6.7			
[Pd(HOPetpE)(PEt_3)](BF_4)$_2$, **6**	58.9	119.8	11.5		9.8	296.5	31.7	
etpEPO, **7**	−18.5	−16.8		31.8	22.9			44.8
[Pd(etpEPO)(CH_3CN)](BF_4)$_2$, **8**	61.1	117.8		29.6	6.5			45.0
				29.5				50.3
[Pd(etpEPO)(PEt_3)](BF_4)$_2$, **9a**	55.2	119.4	10.2	28.9	10.4	304.7	31.7	43.3
				27.9				61.6
[Pd(etpEPO)($P(OMe)_3$)](BF_4)$_2$, **9b**	58.7	117.0	108.6	29.4	12.8	508.1	38.2	48.2
				28.9				55.0
[Pd(etpEPO)($P(CH_2OH)_3$)](BF_4)$_2$, **9c**	58.1	123.7	10.2	30.1	10.1	285.9	32.7	44.4
				29.4				63.5
[Pd(etpEPO)(PPh_3)](BF_4)$_2$, **9d**	48.8	116.1	6.5	25.2	11.8	306.5	23.9	
				22.4				
MNetpE	−17.8	63.3			24.7			
[Pd(MNetpE)(CH_3CN)](BF_4)$_2$, **10a**	61.8	156.8			7.4			
[Pd(MNetpE)(PEt_3)](BF_4)$_2$, **12a**	56.1	161.0	10.9		12.7	316.3	31.9	
IPNetpE, **1**	−17.7	36.1			24.1			
[Pd(IPNetpE)(CH_3CN)](BF_4)$_2$, **10b**	66.2	144.9			5.5			
[Pd(IPNetpE)(PEt_3)](BF_4)$_2$, **12b**	58.4	153.2	20.4		11.0	318.4	31.8	
etpMN	96.4	−15.9			34.1			
[Pd(etpMN)(CH_3CN)](BF_4)$_2$, **11**	124.7	109.4			15.0			
[Pd(etpMN)(PEt_3)](BF_4)$_2$, **13**	129.1	105.8	19.0		13.2	275.9	32.7	

[a] All chemical shifts are reported relative to phosphoric acid as an external reference in acetonitrile-d_3 solutions. P_C, P_T, and P_A refer to the central, terminal, and phosphonate phosphorus atoms of the triphosphine ligands, respectively, and P_L refers to the phosphorus atom of the monodentate ligand.

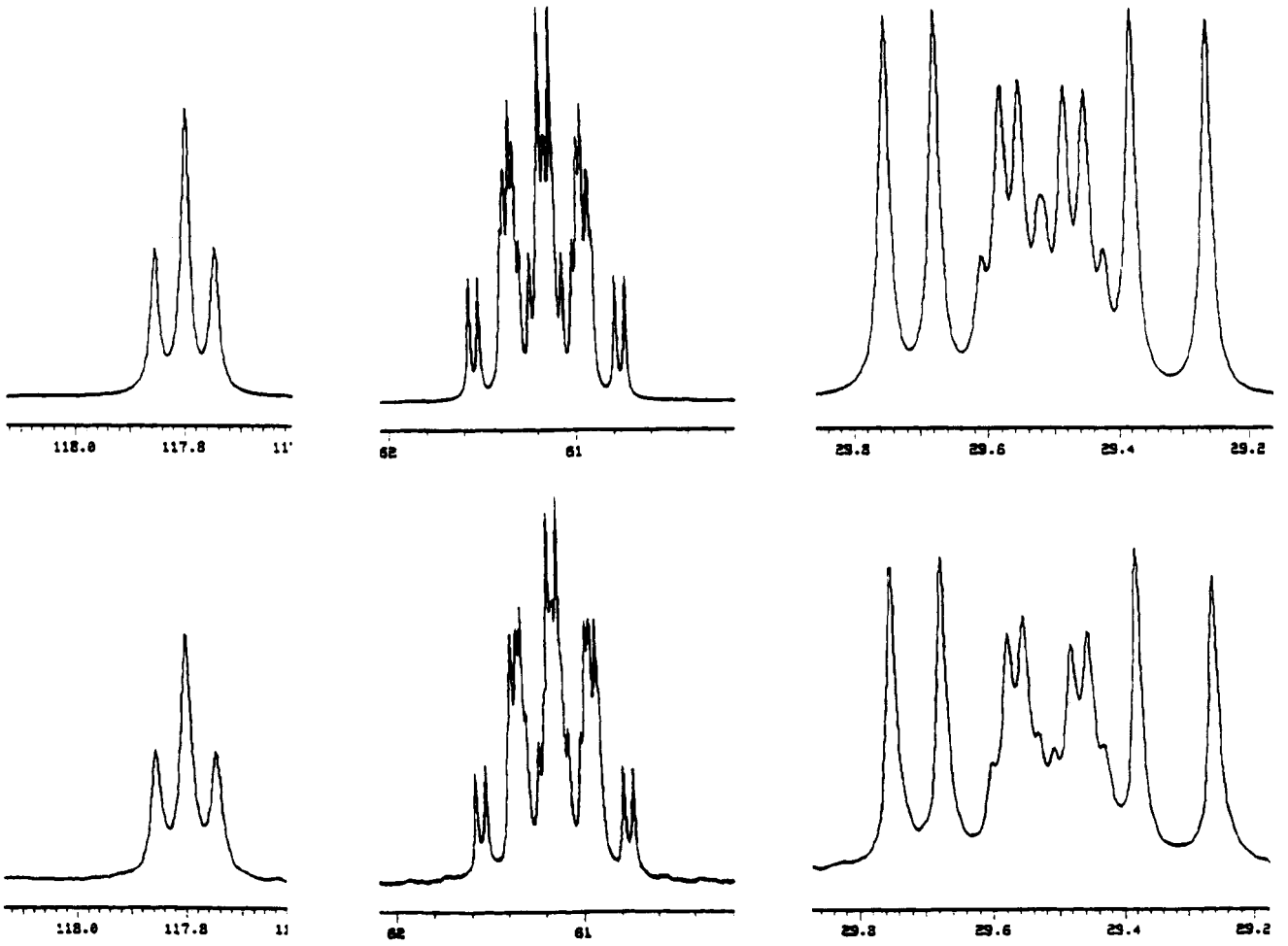

Figure 1. Experimental (bottom) and calculated (top) ^{31}P NMR spectra of [Pd(etpEPO)(CH_3CN)](BF_4)$_2$. Parameters used in the simulation are given in Table 1.

steric interactions between the bulky phosphonate substituents and triphenylphosphine. ^1H NMR spectral data and analytical data for these complexes are given in the Experimental Section. The ^{31}P spectra of these complexes were simulated as described

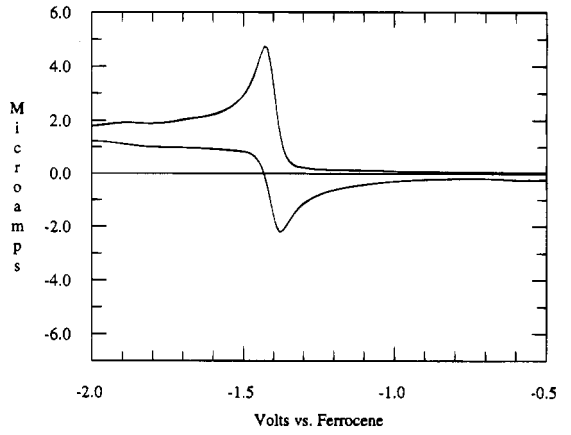

Figure 2. Cyclic voltammogram of a 2.2 × 10^{-3} M solution of [Pd(HOPetpE)(PEt$_3$)](BF$_4$)$_2$ in dimethylformamide (0.2 M NEt$_4$BF$_4$). The scan rate was 50 mV/s, and the working electrode was glassy carbon. Potentials are referenced to ferrocene.

above for the acetonitrile complex and gave fits comparable to that shown in Figure 1. The parameters used in the simulations are listed in Table 1.

Dialkylamino-substituted triphosphine ligands can be prepared using modifications of methods developed by King and coworkers for closely related triphosphine ligands.[14] A representative preparation is shown in the first step of Scheme 1. Spectroscopic data for these ligands are summarized in Table 1 and the Experimental Section. Reaction of these ligands with with [Pd(CH$_3$CN)$_4$](BF$_4$)$_2$ forms complexes **10a**, **10b**, and **11**.

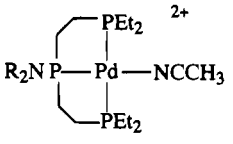

	R
10a	Me
10b	*i*-Pr

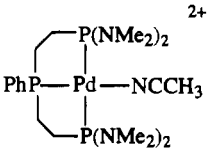

11

Complexes **10a** and **11** are hygroscopic and water soluble. The spectroscopic data for these complexes are given in Table 1 and in the Experimental Section. As for complexes **5** and **8**, the acetonitrile ligands of **10a**, **10b**, and **11** are labile and readily substituted by triethylphosphine to form the analogous triethylphosphine complexes **12a**, **12b**, and **13**.

Electrochemical Studies. A quasi-reversible reduction at −1.40 V vs the ferrocene/ferrocenium couple is observed for [Pd(HOPetpE)PEt$_3$](BF$_4$)$_2$, **6**, as can be seen from the cyclic voltammogram shown in Figure 2. A linear plot of the peak current vs the scan rate between 20 and 400 mV/s indicates a diffusion-controlled reduction.[15] The peak-to-peak separation of 49 mV and an $E_p - E_{p/2}$ value of 37 mV at a scan rate of 50 mV/s are consistent with a two-electron reduction with a somewhat sluggish electron transfer rate.[16] The ratio of the anodic peak current to the cathodic peak current was 0.7. A ratio of less than 1.0 suggests a chemical reaction following the initial reduction.[16] This reaction is not a loss of triethylphosphine, because the addition of excess triethylphosphine does not increase this ratio. Controlled-potential electrolysis of **6** at −1.5 V resulted in the passage of 1.1 electrons and the formation of the Pd(I) dimer **14.** This structural assignment

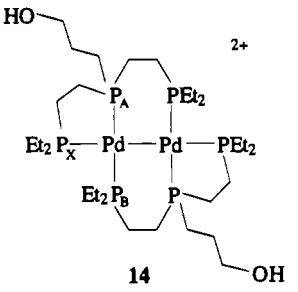

14

for the reduction product is based on the close similarity of the cyclic voltammograms, UV−vis spectra, and ^{31}P NMR spectra of the reduced solution (see the Experimental Section) to those of analogous Pd(I) dimers characterized by X-ray diffraction studies.[4] In particular, compound **14** exhibits an AA′BB′XX′ ^{31}P NMR spectrum characteristic of these dimers with a large trans coupling between P_A and P_B. Compound **14** can also be prepared by a comproportionation reaction between [Pd(CH$_3$CN)$_4$](BF$_4$)$_2$ and [Pd$_2$(dba)$_3$] (where dba is dibenzylideneacetone) in the presence of the triphosphine ligand. A plausible mechanism for the formation of **14** is the reduction of [Pd(HOPetpE)PEt$_3$](BF$_4$)$_2$ by two electrons followed by comproportionation with unreduced [Pd(HOPetpE)PEt$_3$](BF$_4$)$_2$.

The cyclic voltammograms of the other complexes containing monodentate phosphine ligands also exhibit simple reversible or quasi-reversible two-electron reductions, and the data for these complexes are summarized in Table 2. For [Pd(etpEPO)PEt$_3$](BF$_4$)$_2$, the only detectable product formed by controlled-potential electrolysis is [Pd(etpEPO)PEt$_3$]. This assignment is based on the amount of charge passed during electrolysis (1.84 faradays/mol) and the ^{31}P NMR spectrum of the reduced solution (see the Experimental Section). In general, the quantities of charge passed during controlled potential reductions of the triethylphosphine complexes range between one and two Faradays per mole of complex, and the ^{31}P NMR spectra of the reduced solutions indicate a mixture of products.

As shown by trace a of Figure 3, the reduction of [Pd(HOPetpE)(CH$_3$CN)](BF$_4$)$_2$, **5**, is not a reversible process. A plot of the peak current versus the square root of the scan rate for the cathodic wave at −1.54 V is linear between 50 and 400 mV/s, indicating a diffusion-controlled reduction over this range. Controlled-potential electrolysis carried out at −1.6 V resulted in the passage of 1.2 faradays/mol of complex, suggesting a one-electron reduction. However, comparison of the chronocoulometric results for **5** and **6** suggests that the cathodic wave at −1.54 V actually involves two closely spaced one-electron reductions. The slope of the plot of the charge versus the square root of time for **5** was 74% of the slope of its triethylphosphine analogue, **6**, which undergoes a quasi-reversible two-electron reduction. This corresponds to a transfer of 1.5 faradays/mol. On the longer time scale of the bulk electrolysis experiment, only one electron is passed. During the controlled-potential electrolysis of **5**, any Pd(0) formed during the initial electron transfer step may undergo a comproportionation reaction with **5** present in the bulk solution to form the Pd(I) species **14** observed at the end of the electrolysis. On the shorter time scale of the chronocoulometry experiment, both Pd(0) and Pd(I) species are formed, because the Pd(0) species formed initially do not have sufficient time to undergo comproportionation with the bulk Pd(II) species. The electrochemical behaviors of the acetonitrile complexes, **8**, **10**, and **11**, are similar to that of **5**, and the data for these complexes are summarized in Table 2.

(14) King, R. B.; Master, W. F. *J. Am. Chem. Soc.* **1977**, *99*, 4001−4008.
(15) Fry, A. J. *Synthetic Organic Electrochemistry*; Wiley: New York, 1989; pp 25, 31.
(16) Bard, A. J.; Faulkner, L. R. *Electrochemical Methods*; Wiley: New York, 1980; pp 219, 229. Nicholson, R. S.; Shain, I. *Anal. Chem.* **1964**, *36*, 706−723.

Table 2. Electrochemical Data

compound	E_p ($E_{1/2}$),[a] V	ΔE_p ($E_p - E_{p/2}$),[b] mV	i_{pa}/i_{pc}[c]	n[d]	k_1, [e] M^{-1} s^{-1}	cur eff,[f] % DMF	cur eff,[f] % H_2O	turnover no.[g]
[Pd(HOPetpE)($NCCH_3$)](BF_4)$_2$, **5**	−1.54	(94)	0.3	1.2	309	49	40	10
[Pd(HOPetpE)(PEt_3)](BF_4)$_2$, **6**	(−1.40)	48 (38)	0.7	1.1				
[Pd(etpEPO)($NCCH_3$)](BF_4)$_2$, **8**	−1.50	(73)	0	1.0	71	39	17	3
[Pd(etpEPO)(PEt_3)](BF_4)$_2$, **9a**	(−1.25)	193 (82)	1.0	1.8				
[Pd(etpEPO)($P(OMe)_3$)](BF_4)$_2$, **9b**	(−1.18)	442 (180)	0.3					
[Pd(etpEPO)$P(CH_2OH)_3$](BF_4)$_2$, **9c**	(−1.27)	316 (84)	0.5	1.3				
[Pd(IPNetpE)($NCCH_3$)](BF_4)$_2$, **10b**	(−1.35)	197 (91)	0.6	1.5	57	78		4
[Pd(IPNetpE)(PEt_3)](BF_4)$_2$, **12b**	(−1.25)	64 (34)	0.8	0.8				
[Pd(MNetpE)($NCCH_3$)](BF_4)$_2$, **10a**	−1.64	(140)	0	1.6	100	23	6	1
[Pd(MNetpE)(PEt_3)](BF_4)$_2$, **12a**	(−1.40)	46 (59)	0.6	1.5				
[Pd(etpMN)($NCCH_3$)](BF_4)$_2$, **11**	−1.38	(63)	0	0.9	113	31	0	2
[Pd(etpMN)(PEt_3)](BF_4)$_2$, **13**	(−1.30)	36 (38)	0.4	1.8				

[a] E_p and $E_{1/2}$ (values in parentheses) are the peak and half-wave potentials, respectively, of the first cathodic wave. All potentials are referenced to the ferrocene/ferrocenium couple. [b] ΔE_p is the difference in potential between the cathodic and anodic peaks. $E_p - E_{p/2}$ is the difference between the potential of the peak of the first cathodic wave and the potential at half-height. [c] i_{pa}/i_{pc} is the ratio of the anodic peak current to the cathodic peak current for the first cathodic wave. [d] n is the number of faradays passed per mole of complex in controlled-potential electrolysis experiments carried out at potentials approximately 100 mV negative of the cathodic peak potential. [e] k_1 is the rate constant for the reaction of Pd(I) with CO_2. This constant was calculated from the catalytic current as discussed in the text. [f] The current efficiencies were calculated assuming that two electrons were required for each mole of CO and H_2 produced. The error in each measurement is estimated to be about 5%. [g] The turnover numbers are based on the number of moles of CO produced per mole of catalyst when the catalytic current had decayed to approximately 10% of its initial value.

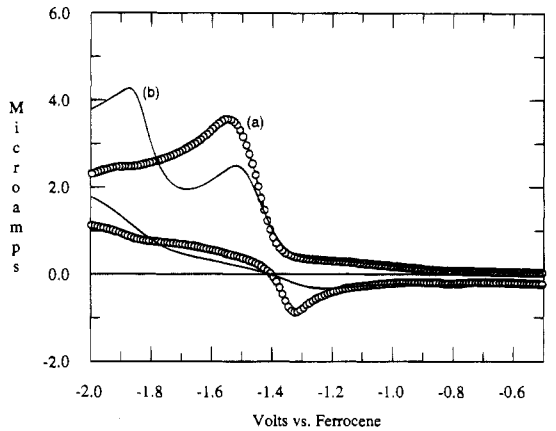

Figure 3. (a) Cyclic voltammogram of a 2.5 × 10^{-3} M solution of [Pd(HOPetpE)(CH_3CN)](BF_4)$_2$ in dimethylformamide under nitrogen (open circles). (b) Cyclic voltammogram of same solution saturated with CO_2 at 620 mm Hg (0.18 M). The scan rate was 100 mV/s.

Trace b in Figure 3 shows the effect of adding CO_2 to a dimethylformamide solution of **5**. It can be seen that the current of the cathodic wave at −1.54 V is decreased in the presence of CO_2, and the peak potential shifts in a positive direction. A new wave is also observed at −1.87 V. These effects are attributed to a fast reaction of CO_2 with a transient monomeric Pd(I) intermediate. The decrease in the wave at −1.54 V results from a change in the nature of this wave from two, closely spaced, one-electron reductions to a simple one-electron reduction followed by a fast chemical reaction with CO_2. The reaction with CO_2 prevents further reduction to Pd(0). This interpretation is supported by comparing chronocoulometric experiments of **5** under N_2 and CO_2. The slope of the plot of charge vs the square root of time under CO_2 is 51% of that for the triethylphosphine complex, **6**, which undergoes a two-electron reduction. These data support a simple one-electron reduction for **5** in the presence of CO_2. The new wave that appears at −1.87 V is tentatively assigned to the reduction of a new CO_2 complex formed by reaction of CO_2 with a transient Pd(I) monomer.

Figure 4a shows cyclic voltammograms of acidic DMF solutions of **5** purged with CO_2 (open circles) and N_2 (solid line). The increased current observed in the presence of CO_2 is attributed to the catalytic reduction of CO_2. Controlled-potential electrolysis at −1.6 V of DMF solutions containing 0.1 M HBF_4, 1.0 × 10^{-3} M **5**, and 0.18 M CO_2 resulted in the production of CO (49%) and H_2 (54%). Within experimental error (approximately 5%), these two products account for all of the charge passed during the electrolysis. These results indicate that carbon monoxide is the product of CO_2 reduction.

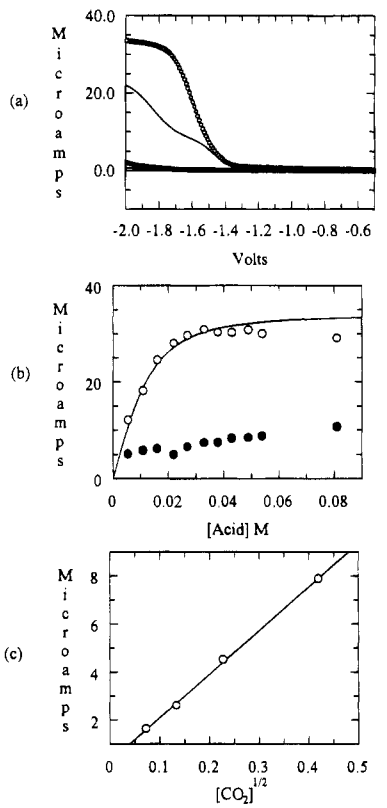

Figure 4. (a) Cyclic voltammograms of a 2.5 × 10^{-3} M solution of [Pd(HOPetpE)(CH_3CN)](BF_4)$_2$ in dimethylformamide containing 0.056 M HBF_4 under nitrogen (solid line) and saturated with CO_2 (open circles). (b) Dependence of current on acid concentration for a 2.5 × 10^{-3} M solution of [Pd(HOPetpE)(CH_3CN)](BF_4)$_2$ in dimethylformamide under CO_2 (open circles) and nitrogen (solid circles) atmospheres. The solid curve is a plot of eq 2 with k_1 = 370 M^{-1} s^{-1} and k_2 = 2.5 × 10^5 M^{-2} s^{-1}. (c) Plot of the catalytic current versus the square root of the CO_2 concentration. Open circles are data points, and the solid line is the best fit line.

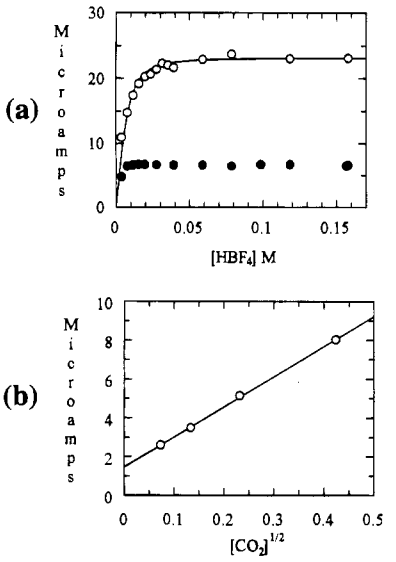

Figure 5. (a) Plot showing dependence of the catalytic current on the concentration of HBF_4 for a 2.2×10^{-3} M solution of [Pd(IPNetpE)(CH_3CN)](BF_4)$_2$ in dimethylformamide purged with N_2 (solid circles) and CO_2 (open circles). The solid line is a plot of eq 2 with $k_1 = 57$ M^{-1} s^{-1} and $k_2 = 1.1 \times 10^5$ M^{-2} s^{-1}. (b) Plot of the catalytic current versus the square root of the CO_2 concentration for a 0.7×10^{-3} M solution of [Pd(IPNetpE)(CH_3CN)](BF_4)$_2$ in dimethylformamide containing 0.1 M HBF_4.

Plots b and c in Figure 4 show the dependence of the catalytic current on the concentrations of CO_2 and acid. In the presence of CO_2 (0.18 M), the catalytic current exhibits a biphasic dependence on the acid concentration as shown in Figure 4b (open circles). At low acid concentrations, a first-order dependence is observed, while no dependence is observed at high acid concentrations. This relationship between current and acid concentration implies a rate-determining step that is second order in $[H^+]$ at low acid concentrations and zero order in $[H^+]$ at high acid concentrations. At high acid concentrations, the catalytic current has a square root dependence on the CO_2 concentration, which implies a first-order dependence on CO_2 of the rate-determining step. Figure 5 shows that the catalytic current of [Pd(IPNetpE)(CH_3CN)](BF_4)$_2$ has the same qualitative dependence on CO_2 and acid as does that of [Pd(HOetpE)(CH_3CN)](BF_4)$_2$. This is true of the other acetonitrile complexes as well. These experimental data can be fit to eq 2, which has been used previously for other [Pd(triphosphine)(solvent)](BF_4)$_2$ complexes.[4]

$$\frac{i_c}{i_d} = \frac{\sigma}{0.447}\sqrt{\frac{RT}{nFv}}\sqrt{\frac{k_1 k_2 [CO_2][H^+]^2}{k_1[CO_2] + k_2[H^+]^2}} \qquad (2)$$

Equation 2 allows the rate constants for the catalytic reaction to be calculated, although the values of these constants depend on whether the second electron transfer occurs at the electrode surface or in solution.[17] Assuming that the second electron transfer occurs at the electrode surface leads to rate constants that are a factor of 2 smaller than if one assumes a solution electron transfer. In this and previous work,[4] we have used this more conservative estimate of the reaction rate. The solid lines shown in Figures 4 and 5 for [Pd(HOPetpE)(CH_3CN)](BF_4)$_2$ and [Pd(IPNetpE)(CH_3CN)](BF_4)$_2$ were calculated using eq 2, and the k_1 and k_2 values are given in the figure captions.

(17) Savéant, J.-M.; Su, K. B. *J. Electroanal. Chem. Interfacial Electrochem.* **1985**, *196*, 1−22. Savéant, J.-M.; Vianello, E. *Electrochim. Acta* **1965**, *10*, 905−920.

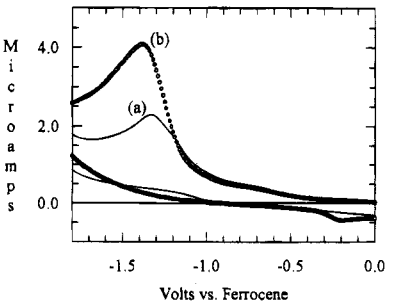

Figure 6. Cyclic voltammograms of a 2.4×10^{-3} M solution of [Pd(HOPetpE)(CH_3CN)](BF_4)$_2$ in water (0.1 M NEt_4BF_4) under nitrogen (a) and purged with CO_2 (b).

The rate constant k_2 is assumed to be a composite constant with contributions from more than one elementary chemical step. The values of the catalytic rate constants and current efficiencies for all of the acetonitrile complexes are summarized in Table 2. Although some of the complexes containing monodentate phosphines exhibit catalytic activity, their activities are reduced compared to those of the acetonitrile complexes. This is consistent with our previous observation that monodentate phosphine ligands inhibit the catalytic reaction.[4]

Electrochemical Studies in Water and Mixed Water−DMF Solutions. The cyclic voltammogram of **5** in water is shown in Figure 6 trace a. It can be seen that the reduction wave under nitrogen is irreversible and similar to that of the reduction observed in DMF (Figure 3 trace a). This wave is diffusion controlled between 10 and 1000 mV/s as indicated by a square root dependence of the peak current on the scan rate.[15] In the presence of CO_2, this wave increases in height as shown in trace b of Figure 6. This behavior is different from that observed in DMF, but not unexpected. In DMF, there are no protons available for protonation of the bound CO_2 in the absence of added acid, and the current decreases because of the rapid reaction of the one-electron-reduction product with CO_2 before a second electron transfer can take place. In water, the availability of protons leads to protonation of coordinated CO_2 and a catalytic wave. Controlled-potential electrolysis of an aqueous solution of **5** under CO_2 results in a low current efficiency for the production of CO (approximately 2%). Unbuffered solutions of **5** quickly become basic, and the catalyst is rapidly deactivated. In phosphate-buffered solutions, the performance of **5** is improved, and the current efficiency of approximately 40% is comparable to that observed in acidic DMF solutions. Table 2 summarizes the current efficiencies for CO production in DMF and water for **5** and other complexes described above. It can be seen that several of the compounds show moderate selectivity for CO formation in water, although the current efficiencies in DMF are higher. This may be caused in part by the much higher solubility of CO_2 in DMF compared with its solubility in water.[18] This simple explanation is somewhat complicated by the different acid strengths of these solutions. Increasing the acidity of the aqueous solutions results in a loss in selectivity for CO production. When H_3PO_4 (0.05 M) or HBF_4 (0.11 M) is used as an acid in aqueous solutions of **5**, no CO production is observed. Results of studies on the current efficiencies of other complexes in DMF and buffered aqueous solutions are also summarized in Table 2.

Using eq 2 to calculate catalytic rate constants in water for these complexes is problematic. Only in solutions buffered at

(18) *Solubilities of Inorganic and Organic Compounds*; Stephen, H., Stephen, T., Eds.; Pergamon: New York, 1958; Vol. 1, p 1063. Palmer, D. A.; Van Eldik, R. *Chem. Rev.* **1983**, *83*, 653−654. Wilhelm, E.; Battino, R.; Wilcock, R. *Chem. Rev.* **1977**, *77*, 219−262. Malin, S. D. *Geochem. Int.* **1979**, *15* (5), 108−119.

approximately pH 7 is significant selectivity for CO observed. Consequently, it was not possible to determine the acid dependence of the catalytic reaction in water, and the magnitude of the catalytic current at pH 7 is small, which prevented an accurate determination of the current dependence on CO_2 concentration. Because of these complications, rate constants could not be measured in water.

Discussion

Water-soluble analogues of [Pd(triphosphine)(CH_3CN)](BF_4)$_2$ complexes shown previously to catalyze the electrochemical reduction of CO_2 to CO have been prepared by modifying both the terminal and central phosphorus atoms of the triphosphine with polar substituents. The central phosphorus atom has been modified with hydroxypropyl and dialkylamino functional groups, and the terminal phosphorus atoms have been modified with (diethoxyphosphoranyl)ethyl and dialkylamino substituents. These triphosphine ligands react with [Pd(CH_3CN)$_4$](BF_4)$_2$ forming water-soluble [Pd(triphosphine)(CH_3CN)](BF_4)$_2$ complexes. The order of solubility of the acetonitrile complexes in water is [Pd(etpEPO)(CH_3CN)](BF_4)$_2$ > [Pd(etpMN)(CH_3CN)](BF_4)$_2$ > [Pd(HOPetpE)(CH_3CN)](BF_4)$_2$, [Pd(MNetpE)(CH_3CN)](BF_4)$_2$ > [Pd(IPNetpE)(CH_3CN)](BF_4)$_2$. The ligand etpEPO and its complex, [Pd(etpEPO)(CH_3CN)](BF_4)$_2$, are very soluble in water, while [Pd(IPNetpE)(CH_3CN)](BF_4)$_2$ is only slightly soluble in water. The synthetic strategies used to generate water-soluble complexes containing triphosphine ligands extend previous work on monodentate and bidentate ligands.[13,14]

The labile acetonitrile ligand in the [Pd(triphosphine)(CH_3CN)](BF_4)$_2$ complexes can be easily substituted with monodentate phosphine ligands. In general, the substituents on the triphosphine ligand do not appear to affect the coordination sphere around palladium in any significant fashion. However, the coordination of phosphine ligands to [Pd(etpEPO)(CH_3CN)](BF_4)$_2$ appears to be more difficult for the larger triphenylphosphine ligand than for triethylphosphine or trimethyl phosphite, which suggests a significant steric interaction with the diethyl phosphonate substituents of the etpEPO ligand.

[Pd(triphosphine)(PR_3)](BF_4)$_2$ complexes studied previously undergo reversible or quasi-reversible two-electron reductions. The corresponding [Pd(triphosphine)(CH_3CN)](BF_4)$_2$ complexes undergo two, closely spaced, one-electron reductions with small or no associated oxidation waves.[4] The compounds shown in Table 2 exhibit similar behavior. Those containing monodentate phosphine ligands exhibit ΔE_p values between 36 and 442 mV. For a truly reversible two-electron reduction, a ΔE_p value of approximately 30 mV is expected.[16] The larger values observed for the complexes listed in Table 2 are indicative of somewhat sluggish electron transfer rates, which are attributed to the reorganization that must accompany the reduction from a square planar Pd(II) species to a tetrahedral Pd(0) species. The [Pd(etpEPO)(PR_3)](BF_4)$_2$ complexes, **9a-c,** have the largest values of ΔE_p, which suggests a slower interconversion between these two geometries because of steric interactions between the bulky diethyl phosphonate substituents on the etpEPO ligand and the monodentate phosphine.

The shift of the peak potential and the decrease in the peak height observed for the cyclic voltammograms of [Pd(HOPetpE)(CH_3CN)](BF_4)$_2$, **5**, in the presence of CO_2 compared to nitrogen (Figure 3) are consistent with a rapid reaction of a Pd(I) intermediate with CO_2. At high acid concentrations, **5** exhibits catalytic currents that have a square root dependence on the CO_2 concentration. Both of these results suggest that the reaction of a monomeric Pd(I) species with CO_2 to form a Pd(I)-CO_2 intermediate is the rate-determining step at high acid concentrations (reaction 3). This Pd(I)−CO_2 intermediate reacts

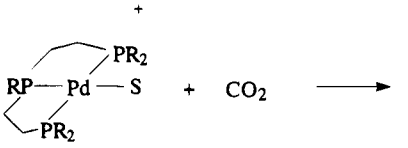

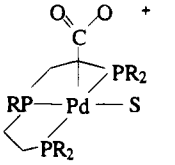

(3)

with protons in solution and picks up an additional electron to produce either CO or hydrogen. At low acid concentrations, the rate-determining step exhibits a second-order dependence on acid concentration, consistent with two protons being bound in the transition state. Under these conditions, the rate-determining step is likely the cleavage of the C−O bond, producing CO and H_2O as shown in step 2 of reaction 4.

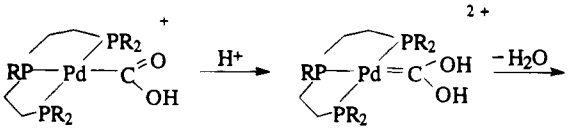

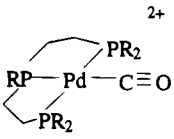

(4)

Precedent for this reaction can be found in the protonation of isolated hydroxy and methoxy carbonyls of Pt to produce CO.[19] These results are consistent with the mechanism proposed previously for other [Pd(triphosphine)(CH_3CN)](BF_4)$_2$ complexes in dimethylformamide[4] and demonstrate that the substituents introduced on the triphosphine ligand have no effect on the mechanism of CO_2 reduction. Also supporting this conclusion is the observation that the rate constants shown in Table 2 are in the range expected. Unfortunately, for experimental reasons cited above, mechanistic studies on these complexes could not be carried out in water.

The current efficiencies in DMF range from 78% to 23%. The selectivity decreases somewhat for aqueous solutions as shown in Table 2, but for [Pd(HOPetpE)(CH_3CN)](BF_4)$_2$, this decrease is not significant. This result is surprising because the solubility of CO_2 is significantly lower in water than in dimethylformamide. Unfortunately, the complex with the highest selectivity in DMF, [Pd(IPNetpE)(CH_3CN)](BF_4)$_2$, is not sufficiently soluble in water to be evaluated. The selectivity in aqueous solutions is sensitive to pH. When solutions of **5** were electrolyzed in the presence of either phosphoric acid or tetrafluoroboric acid, no CO production was observed. However, the results presented here for buffered solutions clearly indicate the feasibility of carrying out CO_2 reduction in aqueous solutions with [Pd(triphosphine)(CH_3CN)](BF_4)$_2$ catalysts.

The final column in Table 2 shows the turnover numbers for the catalysts in DMF. The turnover numbers shown are

(19) Bennet, M. A.; Robertson, G. B.; Rokicki, A.; Wickramasinghe, W. A. *J. Am. Chem. Soc.* **1988**, *110*, 7098−7105. Byrd, J. E.; Halpern, J. *J. Am. Chem. Soc.* **1971**, *93*, 1634. Clark, H. C.; Jacobs, W. J. *Inorg. Chem.* **1970**, *9*, 1229. Bertani, R.; Mozzon, M.; Michelin, R. A.; Benetollo, F.; Bombieri, G.; Castilho, T. J.; Pombeiro, J. L. *Inorg. Chim. Acta* **1991**, *189*, 175−187.

calculated on the basis of the number of moles of CO formed per mole of catalyst before the current decayed to less than 10% of its original value. Clearly these catalysts are rather fragile. This decomposition is not caused by the instability of the catalyst under catalytic conditions, because the catalysts remain unchanged after several hours in solution if no current is passed. For some catalysts, the decomposition product is known. For example, the complexes $[Pd(HOPetpE)(CH_3CN)](BF_4)_2$ and $[Pd(etpEPO)(CH_3CN)](BF_4)_2$ form dimeric Pd(I) species similar to **14** on reduction. In other cases, the fates of the catalysts were not determined.

Summary

Water-soluble $[Pd(triphosphine)(CH_3CN)](BF_4)_2$ complexes have been prepared and characterized. Kinetic studies carried out in DMF solutions indicate that the mechanism of CO_2 reduction is the same as that proposed previously for complexes without water-soluble functional groups. Two of the complexes exhibit catalytic activity for CO_2 reduction in buffered aqueous solutions, illustrating the feasibility of using this class of compounds in water. In addition, the ligands described above may have applications in other catalytic processes in which water solubility is an important consideration.

Experimental Section

Physical Measurements and General Procedures. ^1H and ^{31}P NMR spectra were recorded on a Varian Unity 300-MHz spectrometer at 299.75 and 121.42 MHz, respectively. ^1H chemical shifts are reported relative to tetramethylsilane using residual solvent protons as a secondary reference. ^{31}P chemical shifts are reported relative to external phosphoric acid. Infrared spectra were recorded on a Nicolet 510P spectrometer. Simulations of ^{31}P NMR spectra for compounds containing the etpEPO ligand were carried out with Varian VNMR software revision 3.2A using a program based on LAOCOON.[20] Elemental analyses were performed by Schwarzkopf Laboratories, Woodside, NY. Elemental analyses were not obtained for the triphosphine ligands due to their air sensitivity, toxicity, and viscosity. Analytical data were obtained for the metal complexes which serve as derivatives of the ligands. From ^1H and ^{31}P NMR data we estimate that all ligands have purities greater than 90%. All syntheses were carried out using standard Schlenk and drybox techniques.

Cyclic voltammetry experiments were carried out on a Cypress Systems computer-aided electrolysis system equipped with a CYSY 1r potentiostat. The working electrode was a glassy carbon disk (1-mm diameter, Cypress Systems). The counter electrode was a glassy carbon rod (1-mm diameter), and a platinum wire immersed in an acetonitrile solution containing 1.5×10^{-3} M permethylferrocene and 1.5×10^{-3} M permethylferrocenium tetrafluoroborate was used to establish a reference potential.[21] Ferrocene was used as an internal standard, and all potentials are referenced to the ferrocene/ferrocenium couple.[22] Controlled-potential experiments were performed with a Princeton Applied Research Model 173 potentiostat equipped with a Model 179 digital coulometer and a Model 175 universal programmer. Working electrodes were constructed from reticulated vitreous carbon cylinders (60 pores/in., Electrosynthesis Corp., 14-mm diameter). Electrical contact between the copper lead and the reticulated vitreous carbon was made with silver epoxy (Johnson Matthey). These electrodes were inserted to a depth of 10 mm in the solutions to be electrolyzed. The counter electrode was a tungsten wire. A silver wire immersed in an acetonitrile solution containing 1.5×10^{-3} M permethylferrocene and 1.5×10^{-3} M permethylferrocenium tetrafluoroborate was used to establish a reference potential.[21] The reference and counter electrodes were separated from the working electrode compartment by Vycor frits (7-mm diameter, 1-mm thick). All electrochemical experiments were carried out in 0.1 M Et_4NBF_4–dimethylformamide solutions unless otherwise noted. In a typical electrolysis experiment, the potential of the working electrode was held at a value approximately 100 mV negative of the first cathodic wave, and the charge consumed was measured after the current had decayed to <5% of its initial value. An example is given below following the preparation of $[Pd(HOPetpE)(CH_3CN)](BF_4)_2$.

Measurements of current efficiencies for gas production were carried out in a sealed flask from which gas aliquots were withdrawn for gas chromatographic analysis. Details of chromatography conditions are presented elsewhere.[23] In a typical experiment, a 1.0×10^{-3} M solution of catalyst in dimethylformamide (10.0 mL) was saturated with CO_2 by purging the solution for approximately 30 min. HBF_4 (50 μL, 9.4 M) was added via syringe, and the solution was electrolyzed at potentials approximately 100 mV negative of the first cathodic wave of the catalyst. Similar experiments were carried out in buffered aqueous solution containing 0.1 M NEt_4BF_4, 0.3 M NaH_2PO_4, and 0.5 M Na_2HPO_4 (pH = 6.9).

Materials. Allyl alcohol, 2,2′-azobis(2-methylproprionitrile) (AIBN), triphenylphosphine, $Pd_2(dba)_3$, and diethyl vinylphosphonate were purchased from Aldrich. Matheson Bone Dry carbon dioxide was used in all electrolysis experiments. Diethylphosphine, triethylphosphine, and phenylphosphine were purchased from Strem Chemicals and were used as received. Tetrahydrofuran and diethyl ether were distilled from sodium benzophenone ketyl, and acetonitrile was distilled from calcium hydride. Dimethylformamide was purchased from Burdick and Jackson and stored under nitrogen. Et_4NBF_4 was recrystallized from ethanol and dried under vacuum at 100 °C for 1 day. $[Pd(CH_3CN)_4](BF_4)_2$,[24] $P(CH_2OH)_3$,[23] bis(dimethylamino)vinylphosphine,[14] (dimethylamino)-divinylphosphine,[14] and bis[bis(((diethoxyoxophosphoranylethyl)-phosphino)ethyl]phenylphosphine (etpEPO)[12] were prepared by literature methods.

Syntheses. Bis((diethylphosphino)ethyl)(dimethylamino)phosphine, $Me_2NP(CH_2CH_2PEt_2)_2$, MNetpE. A mixture of diethylphosphine (5.0 g, 55.5 mmol), (dimethylamino)divinylphosphine (3.3 g, 25.5 mmol), and AIBN (0.2 g, 1.4 mmol) was stirred in a sealed Schlenk flask and irradiated with both 254- and 350-nm lamps for 6 days in a Rayonet photoreactor. The volatile materials were removed in a vacuum at room temperature. The resulting pale yellow oil (5.25 g, 66%) was distilled under reduced pressure (140–145 °C, 4 Torr) to give a colorless oil (2.2 g, 28%). ^1H NMR (acetonitrile-d_3): $(CH_3)_2N$, 2.56 ppm (d, $^3J_{PH}$ = 8.3 Hz); PCH_2CH_2P, 1.1–1.7 ppm (m); PCH_2CH_3, 1.38 ppm (dq, $^3J_{HH}$ = 7 Hz, $^2J_{PH}$ = 1 Hz); PCH_2CH_3, 1.02 ppm (dt, $^3J_{PH}$ = 13.8 Hz).

Bis((diethylphosphino)ethyl)(diisopropylamino)phosphine, i-$Pr_2NP(CH_2CH_2PEt_2)_2$, IPNetpE, 1. This compound was prepared in 57% yield using a procedure similar to that for MNetpE. ^1H NMR (acetonitrile-d_3): $(CH_3)_2CH$, 3.37 ppm (doublet of septets, $^3J_{HH}$ = 7 Hz, $^3J_{PH}$ = 9.4 Hz); PCH_2CH_2P, 1.3–1.7 ppm (m); PCH_2CH_3, 1.39 ppm (q, $^3J_{HH}$ = 6.6 Hz); $(CH_3)_2CH$, 1.10 ppm (d); PCH_2CH_3, 1.02 ppm (dt, $^3J_{PH}$ = 13.9 Hz).

Bis[(bis(dimethylamino)phosphino)ethyl]phenylphosphine, $PhP[CH_2CH_2P(NMe_2)_2]_2$, etpMN. This ligand has been prepared previously by a slightly different procedure.[14] A mixture of phenylphosphine (2.0 g, 18.2 mmol), bis(dimethylamino)vinylphosphine (6.0 g, 21.0 mmol), and AIBN (0.1 g, 0.7 mmol) was stirred and irradiated in a sealed Schlenk flask for 40 h. The volatile materials were removed with a vacuum, leaving a pale yellow oil (6.5 g, 89%). ^1H NMR (acetonitrile-d_3): Ph, 7.3–7.6 ppm (m); $N(CH_3)_2$, 2.53, 2.57 ppm (d, $^3J_{PH}$ = 6.4 Hz); PCH_2CH_2P, 1.4–1.7 ppm (m).

Bis((diethylphosphino)ethyl)phosphine, $HP(CH_2CH_2PEt_2)_2$, HetpE, 3. H_2O (20 mL, 1.11 mol) was added to a solution of IPNetpE (18.0 g, 49.2 mmol) in THF (50 mL), and the mixture was refluxed for 10

(20) Bothner-by, A. A.; Castellano, S. *J. Chem. Phys.* **1964**, *41*, 3863–3869.
(21) Bashkin, J. K; Kinlen, P. *Inorg. Chem.* **1990**, *29*, 4507–4509. Catellani, M.; Halpern, J. *Inorg. Chem.* **1980**, *19*, 566–568.
(22) Gagne, R. R.; Koval, C. A.; Lisensky, G. C. *Inorg. Chem.* **1980**, *19*, 2854–2855. Gritzner, G.; Kuta, J. *Pure Appl. Chem.* **1984**, *56*, 462–466. Hupp, J. T. *Inorg. Chem.* **1990**, *29*, 5010–5012. Bond, A. M.; McLennan, E. A.; Stojanovic, R. S.; Thomas, F. G. *Anal. Chem.*, **1987**, *59*, 2853–2860.
(23) DuBois, D. L.; Miedaner, A. *J. Am. Chem. Soc.* **1987**, *109*, 113–117. Coskran, K. J.; Verkade, J. G. *Inorg. Chem.* **1965**, *4*, 1655–1657. See also ref 1, second citation.
(24) Sen, A.; Ta-Wang, L. *J. Am. Chem. Soc.* **1981**, *103*, 4627–4629. Hathaway, B. J.; Holah, D. G.; Underhill, A. E. *J. Chem. Soc.* **1962**, 2444–2448.

days. After cooling, the solution was dried overnight with $MgSO_4$ and filtered. The solvent was removed from a small sample of the filtrate for spectral characterization. ^1H NMR (CD_2Cl_2): P(O)*H*, 6.81 ppm (doublet of quintets, $^1J_{PH}$ = 446.6 Hz, $^3J_{HH}$ = 3.5 Hz); H(O)PC*H*$_2$-CH$_2$P, 1.87 ppm (m); H(O)PCH$_2$C*H*$_2$P, 1.62 ppm (m); PC*H*$_2$CH$_3$, 1.42 ppm (q, $^3J_{HH}$ = 7.5 Hz); PCH$_2$C*H*$_3$, 1.01 ppm (dt, $^3J_{PH}$ = 14.0 Hz). The remainder of the filtrate was added slowly to a suspension of $LiAlH_4$ pellets (2.0 g, 53 mmol) in THF (250 mL) at −78 °C. The mixture was then allowed to slowly warm to room temperature and stirred for 2 days. *CAUTION:* Repeated cooling may be necessary to control the evolution of H_2 gas near ambient temperature. The reaction mixture was cooled to 0 °C and slowly hydrolyzed. The suspension was filtered, and the filtrate was dried overnight with $MgSO_4$. After filtration, the solvent was removed with a vacuum to produce a yellow oil. A colorless oil (3.5 g, 27%) was obtained by distillation at reduced pressure (112−116 °C, 3 Torr). ^1H NMR (acetone-d_6): P*H*, 3.21 ppm (doublet of quintets, $^1J_{PH}$ = 192.9 Hz, $^3J_{HH}$ = 6.5 Hz); PC*H*$_2$C*H*$_2$P, 1.46−1.83 ppm (m); PC*H*$_2$CH$_3$, 1.40 ppm (q, $^3J_{HH}$ = 7.5 Hz); PCH$_2$C*H*$_3$, 1.03 ppm (dt, $^3J_{PH}$ = 13.8 Hz). IR (Nujol): ν_{PH} = 2265 cm^{-1}.

Bis((diethylphosphino)ethyl)(hydroxypropyl)phosphine, HOCH$_2$CH$_2$CH$_2$P(CH$_2$CH$_2$PEt$_2$)$_2$, HOPetpE, 4. A mixture of HetpE (3.00 g, 11.3 mmol), allyl alcohol (1.02 g, 17.6 mmol), and AIBN (0.1 g, 0.7 mmol) was irradiated in a sealed Schlenk flask for 3 days. The volatile materials were removed with a vacuum, leaving a pale yellow oil (3.50 g, 95%). ^1H NMR (acetonitrile-d_3): C*H*$_2$OH, 3.49 ppm (t, $^3J_{HH}$ = 6.5 Hz); CH$_2$O*H*, 2.84 ppm (broad singlet); C*H*$_2$C*H*$_2$P, 1.38−1.62 ppm (m); PC*H*$_2$CH$_3$, 1.38 ppm (q, $^3J_{HH}$ = 7.5 Hz); PCH$_2$C*H*$_3$, 1.03 ppm (dt, $^3J_{PH}$ = 14.0 Hz). IR (Nujol): ν_{OH} = 3393 cm^{-1}.

[Pd(HOPetpE)(CH$_3$CN)](BF$_4$)$_2$, 5. An acetonitrile solution (20 mL) of [Pd(CH$_3$CN)$_4$](BF$_4$)$_2$ (2.74 g, 6.17 mmol) was added slowly to an acetonitrile solution (20 mL) of HOPetpE (2.00 g, 6.16 mmol). The yellow solution that resulted was stirred for 1 h and filtered. Slow addition of diethyl ether to the filtrate produced a yellow solid (3.91 g, 98%), which was collected by filtration and dried in a vacuum. Attempts at recrystallization decreased the purity of this compound as judged by ^{31}P NMR spectra and elemental analyses. Anal. Calcd for $C_{17}H_{38}B_2F_8NOPdP_3$·$H_2O$: C, 30.70; H, 6.06; N, 2.10. Found: C, 30.80, 30.77; H, 6.27, 6.08; N, 1.68, 1.63. ^1H NMR (acetonitrile-d_3): C*H*$_2$-OH, 3.56 ppm (broad q, $^3J_{HH}$ = 4.9 Hz); CH$_2$O*H*, ppm (t); C*H*$_2$C*H*$_2$P, 1.6−2.8 ppm (m); PC*H*$_2$CH$_3$, 2.13 ppm (m); PCH$_2$C*H*$_3$, 1.21 ppm (m). IR (Nujol): ν_{CN} = 2298 , 2326 cm^{-1}; ν_{OH} = 3510 cm^{-1}.

[Pd(HOPetpE)]$_2$(BF4)$_2$, 14. A solution of [Pd(CH$_3$CN)$_4$](BF$_4$)$_2$ (0.349 g, 0.786 mmol) in acetonitrile (2 mL) was added by syringe to a solution of HOPetpE (0.51 g, 1.57 mmol) in dichloromethane (5 mL). After the orange solution had been stirred for 1 h, Pd$_2$(dba)$_3$ (0.360 g, 0.393 mmol) was added as a solid. Stirring the initial suspension for 0.5 h resulted in the formation of a dark orange solution. After 18 h, the solution was filtered, and diethyl ether (10 mL) was added to the filtrate. The resulting orange microcrystals (0.61 g, 75%) were collected by filtration and dried in a vacuum. The same product was obtained when a solution of [Pd(HOPetpE)(CH$_3$CN)](BF$_4$)$_2$ (0.057 g, 0.088 mmol) in DMF (10 mL) was electrolyzed at −1.10 V vs FeCp*$_2$ using a reticulated vitreous carbon working electrode. After the current had decayed to <5% of its initial value, the electrolysis was stopped. The charge passed corresponded to 1.2 faradays/mol. ^{31}P NMR (acetonitrile-d_3), AA′BB′XX′ spectrum: central P, 60.2 ppm (d, J = 346 Hz); Et$_2$P (trans to Pd), 43.7 ppm (s); Et$_2$P (trans to P), 26.3 ppm (d). All resonances have additional unresolved splitting. ^1H NMR (acetonitrile-d_3): C*H*$_2$OH, 3.52 ppm (m); CH$_2$O*H*, 2.90 ppm (broad s); PC*H*$_2$, 1.6−2.5 ppm (m); PCH$_2$C*H*$_3$, 1.1 ppm (m). IR (Nujol): ν_{OH} = 3533 cm^{-1}. Electronic absorption spectrum: λ_{max} = 371 nm.

[Pd(HOPetpE)(PEt$_3$)](BF$_4$)$_2$, 6. Triethylphosphine (0.28 g, 2.37 mmol) was added to an acetonitrile solution (10 mL) of [Pd(HOPetpE)-(CH$_3$CN)](BF$_4$)$_2$ (1.00 g, 1.63 mmol), and the reaction mixture was stirred for 1 h. Addition of diethyl ether produced a bright yellow solid (0.85 g, 72%), which was collected by filtration and dried in a vacuum. Anal. Calcd for $C_{21}H_{50}B_2F_8OPdP_4$·0.2Et_2O: C, 35.51; H, 7.00. Found: C, 35.40, 35.35; H, 6.88, 6.83. ^1H NMR (acetonitrile-d_3): C*H*$_2$OH, 3.57 ppm (broad m); Et$_2$O, 3.4 ppm (q); CH$_2$O*H*, 2.97 ppm (broad t); C*H*$_2$C*H*$_2$P, 1.6−2.9 ppm (m); PC*H*$_2$CH$_3$, 2.05 ppm (m); PCH$_2$C*H*$_3$, 1.2 ppm (m). IR (Nujol): ν_{OH} = 3535 cm^{-1}.

[Pd(etpEPO)(CH$_3$CN)](BF$_4$)$_2$, 8. A solution of [Pd(CH$_3$CN)$_4$](BF$_4$)$_2$ (0.69 g, 1.55 mmol) in acetonitrile (25 mL) was added to a stirred solution of etpEPO (1.19 g, 1.57 mmol) in acetonitrile (25 mL). The orange reaction mixture was stirred for 2 h, and then the solvent was removed under vacuum. The yellow solid (1.37 g, 97%) was washed with diethyl ether and dried in a vacuum. Further purification was achieved by recrystallization from a mixture of acetonitrile and diethyl ether. Anal. Calcd for $C_{33}H_{69}B_2F_8O_{15}PdP_8$·0.25$CH_3CN$: C, 33.92; H, 5.93; N, 0.29. Found: C, 33.98, 34.09; H, 6.23, 6.13; N, 0.16, 0.23. ^1H NMR (acetonitrile-d_3): Ph, 7.50−8.10 ppm (m); CH$_3$C*H*$_2$O, 4.06 ppm (m); PC*H*$_2$C*H*$_2$P, 1.75−3.00 ppm (m); C*H*$_3$CN, 1.95 ppm; C*H*$_3$CH$_2$O, 1.29 ppm (overlapping t, $^3J_{HH}$ = 6.9 Hz). IR (CH$_2$Cl$_2$): ν_{CN} = 2312, 2349 cm^{-1}; ν_{PO} = 1237, 1266 cm^{-1}.

[Pd(etpEPO)(PEt$_3$)](BF$_4$)$_2$, 9a. Triethylphosphine (0.080 g, 0.68 mmol) was added via syringe to a solution of [Pd(etpEPO)(CH$_3$CN)]-(BF$_4$)$_2$ (0.50 g, 0.46 mmol) in acetonitrile (25 mL). The yellow reaction mixture was stirred for 2 h, and the solvent was removed under vacuum. The resulting yellow solid (0.450 g, 84%) was washed with diethyl ether and dried in a vacuum. Anal. Calcd for $C_{40}H_{84}B_2F_8O_{12}$-PdP_8·H_2O: C, 36.87; H, 6.65. Found: C, 37.15, 36.88; H, 6.99, 7.08. ^1H NMR (CD$_2$Cl$_2$): Ph, 7.40−7.75 ppm (m); CH$_3$C*H*$_2$OP, CH$_3$C*H*$_2$P 3.90−4.10 ppm (m); PC*H*$_2$C*H*$_2$P, 1.60−3.20 ppm (m); CH$_2$C*H*$_3$, 1.21 ppm (m). IR (Nujol): ν_{PO} = 1233 cm^{-1}.

Electrolysis of [Pd(etpEPO)(PEt$_3$)](BF$_4$)$_2$. [Pd(etpEPO)(PEt$_3$)]-(BF$_4$)$_2$ (0.055 g, 0.043 mmol) in DMF (10 mL) was electrolyzed at −1.20 V vs FeCp*$_2$ using a reticulated vitreous carbon working electrode. After the current had decayed to <5% of its initial value, the electrolysis was stopped. The charge passed corresponded to 1.8 faradays/mol. ^{31}P NMR (acetonitrile-d_3): PEt$_3$, 51.1 ppm (s); P$_T$, 48.1 ppm (dt, $^2J_{PP}$ = 56, 45 Hz); PhP, 40.9 ppm (t); P(O)(OEt)$_2$, 31.1, 31.4 ppm (d, d).

[Pd(etpEPO)P(OCH$_3$)$_3$](BF$_4$)$_2$, 9b. This complex can be prepared in a manner similar to that used for [Pd(etpEPO)(PEt$_3$)](BF$_4$)$_2$ from trimethyl phosphite (0.042 g, 0.34 mmol) and [Pd(etpEPO)(CH$_3$CN)]-(BF$_4$)$_2$ (0.33 g, 0.30 mmol). The product is a yellow solid (0.25 g, 63%). ^1H NMR (acetonitrile-d_3): Ph, 7.50−7.90 ppm (m); P(OCH$_3$)$_3$, 4.2 ppm (d, $^3J_{PH}$ = 11 Hz), CH$_3$C*H*$_2$OP, 4.06 ppm (m); PC*H*$_2$C*H*$_2$P, 1.80−3.00 ppm (m); POCH$_2$C*H*$_3$, 1.26 ppm (m).

[Pd(etpEPO)P(CH$_2$OH)$_3$)](BF$_4$)$_2$, 9c. This complex can be prepared in a manner similar to that used for [Pd(etpEPO)(PEt$_3$)]-(BF$_4$)$_2$ from tris(hydroxymethyl)phosphine (0.065 g, 0.52 mmol) and [Pd(etpEPO)(CH$_3$CN)](BF$_4$)$_2$ (0.40 g, 0.34 mmol). The product is a yellow solid (0.33 g, 75%). Anal. Calcd for $C_{37}H_{78}B_2F_8O_{15}$-PdP_8·2H_2O: C, 33.49; H, 6.23. Found: C, 33.32, 33.51; H, 5.75, 5.79. ^1H NMR (acetonitrile-d_3): Ph, 7.50−7.90 ppm (m); O*H*, 4.98 ppm (broad s); *H*$_2$O 4.40 ppm (broad s); HOC*H*$_2$P, CH$_3$C*H*$_2$OP, 3.60−4.01 ppm (m); PC*H*$_2$C*H*$_2$P, 1.60−3.01 ppm (m); CH$_2$C*H*$_3$, 1.23, 1.27, 1.28 ppm (overlapping t, $^3J_{HH}$ = 7 Hz). IR (Nujol): ν_{OH} (H$_2$O) = 3462 cm^{-1}; ν_{OH} (CH$_2$OH) = 3190 cm^{-1}, ν_{PO} = 1227 cm^{-1}.

Reaction between [Pd(etpEPO)(CH$_3$CN)](BF$_4$)$_2$ and PPh$_3$. PPh$_3$ (0.015 g, 0.057 mmol) was added to a solution of [Pd(etpEPO)(CH$_3$-CN)](BF$_4$)$_2$ (0.050 g, 0.046 mmol) in acetonitrile-d_3 (1 mL), and the mixture was left to stand at room temperature for 4 days. A ^{31}P NMR spectrum of the reaction solution showed that [Pd(etpEPO)(PPh$_3$)](BF$_4$)$_2$ accounted for 60% of the mixture.

[Pd(MNetpE)(CH$_3$CN)](BF$_4$)$_2$, 10a. This compound was synthesized in a fashion similar to that used for [Pd(etpEPO)(CH$_3$CN)](BF$_4$)$_2$ from [Pd(CH$_3$CN)$_4$](BF$_4$)$_2$ (0.72 g, 1.62 mmol) and MNetpE (0.50 g, 1.62 mmol). The product is a yellow solid (0.82 g, 80%). Anal. Calcd for $C_{16}H_{37}B_2F_8N_2PdP_3$: C, 30.48; H, 5.91; N, 4.44. Found: C, 31.19, 31.24; H, 6.30, 6.24; N, 3.81, 3.69. ^1H NMR (acetonitrile-d_3): (C*H*$_3$)$_2$N, 2.82 ppm (d, $^3J_{PH}$ = 10.1 Hz); PC*H*$_2$C*H*$_2$P, 2.0−3.0 ppm (m); PC*H*$_2$-CH$_3$, 2.18 ppm (m); PCH$_2$C*H*$_3$, 1.19 ppm (dt, $^3J_{HH}$ = 7.5 Hz, $^2J_{PH}$ = 2.0 Hz), 1.24 ppm (dt, $^3J_{HH}$ = 7.5 Hz, $^3J_{PH}$ = 2.8 Hz). IR (Nujol): ν_{CN} = 2296, 2325 cm^{-1}.

[Pd(MNetpE)(PEt$_3$)](BF$_4$)$_2$, 12a. This complex was prepared from triethylphosphine (0.048 g, 0.41 mmol) and [Pd(MNetpE)(CH$_3$-CN)](BF$_4$)$_2$ (0.250 g, 0.395 mmol) using a procedure analogous to that for [Pd(etpEPO)(PEt$_3$)](BF$_4$)$_2$. The product is a yellow solid (0.20 g, 73%). Anal. Calcd for $C_{20}H_{49}B_2F_8NPdP_4$: C, 33.95; H, 6.98; N, 1.98. Found: C, 33.97, 33.98; H, 7.17, 7.23; N, 2.27, 2.32. ^1H NMR (acetonitrile-d_3): (C*H*$_3$)$_2$N, 2.74 ppm (d, $^3J_{PH}$ = 10.1 Hz); PC*H*$_2$C*H*$_2$P,

2.0−3.0 ppm (m); P(CH_2CH$_3$)$_2$, 2.14 ppm (m); P(CH_2CH$_3$)$_3$, 2.02 ppm (dt, $^3J_{HH}$ = 7 Hz, $^2J_{PH}$ = 2 Hz); PCH$_2$CH_3, 1.15 ppm (m).

[Pd(IPNetpE)(CH$_3$CN)](BF$_4$)$_2$, 10b. This compound was synthesized in a fashion similar to that used for [Pd(etpEPO)(CH$_3$CN)](BF$_4$)$_2$ from [Pd(CH$_3$CN)$_4$](BF$_4$)$_2$ (0.61 g, 1.37 mmol) and IPNetpE (0.50 g, 1.37 mmol). The product is a yellow solid (0.78 g, 83%). Anal. Calcd for $C_{20}H_{45}B_2F_8N_2PdP_3$: C, 34.99; H, 6.61; N, 4.08; P, 13.53. Found: C, 35.53; H, 6.78; N, 4.07; P, 13.27. ^{1}H NMR (acetonitrile-d_3): (CH$_3$)$_2$CH, 3.75 ppm (d of septets, $^3J_{PH}$ =16.5 Hz, $^3J_{HH}$ = 7 Hz); (CH_3)$_2$CH, 1.25 ppm (d); PCH_2CH_2P, 2.0−3.0 ppm (m); PCH_2CH$_3$, 2.18 ppm (m); PCH$_2$CH_3, 1.19 ppm (dt, $^3J_{HH}$ = 7.5 Hz, $^2J_{PH}$ = 2.0 Hz), 1.24 ppm (dt, $^3J_{HH}$ = 7.5 Hz, $^2J_{PH}$ = 2.8 Hz). IR (Nujol): ν_{CN} = 2296, 2325 cm^{-1}.

[Pd(IPNetpE)(PEt$_3$)](BF$_4$)$_2$, 12b. This complex was prepared in a manner analogous to that used for [Pd(etpEPO)(PEt$_3$)](BF$_4$)$_2$ from triethylphosphine (0.016 g, 0.14 mmol) and [Pd(IPNetpE)(CH$_3$CN)](BF$_4$)$_2$ (0.098 g, 0.15 mmol). The product is a yellow solid (0.078 g, 72%). ^{1}H NMR (acetonitrile-d_3): (CH$_3$)$_2$CH, 3.65 ppm (doublet of septets, $^3J_{HH}$ = 7 Hz, $^3J_{PH}$ = 15.8 Hz); PCH_2CH_2PCH_2CH$_3$, 1.9−3.0 ppm (m); (CH_3)$_2$CH, 1.50 ppm (d); PCH$_2$CH_3, 0.9−1.2 ppm (m).

[Pd(etpMN)(CH$_3$CN)](BF$_4$)$_2$, 11. This compound was prepared in a manner similar to that used for [Pd(etpEPO)(CH$_3$CN)](BF$_4$)$_2$ from [Pd(CH$_3$CN)$_4$](BF$_4$)$_2$ (1.10 g, 2.48 mmol) and etpMN (1.00 g, 2.48 mmol). The product is an orange solid (1.30 g, 73%). An analytically pure sample was obtained by recrystallization from acetonitrile and diethyl ether. Anal. Calcd for $C_{20}H_{40}B_2F_8N_5PdP_3$: C, 33.20; H, 5.57. Found: C, 33.32, 33.51; H, 5.75, 5.79. ^{1}H NMR (acetonitrile-d_3): Ph, 7.6−7.8 ppm (m); N(CH_3)$_2$, 2.67, 2.76 (t, $^3J_{PH}$ = 11.4 Hz); PCH_2CH_2P, 1.76, 2.46, 2.7−2.9 ppm (m). IR (Nujol): ν_{CN} = 2292, 2321 cm^{-1}.

[Pd(etpMN)(PEt$_3$)](BF$_4$)$_2$, 13. This compound was prepared in a manner similar to that used for [Pd(etpEPO)(PEt$_3$)](BF$_4$)$_2$ from triethylphosphine (0.04 g, 0.34 mmol) and [Pd(etpMN)(CH$_3$CN)](BF$_4$)$_2$ (0.20 g, 0.28 mmol). The product is a yellow solid (0.17 g, 76%). Anal. Calcd for $C_{20}H_{40}B_2F_8N_4PdP_4$·1.5Et$_2$O: C, 36.66; H, 6.51; N, 6.58. Found: C, 36.41, 36.40; H, 6.64, 6.67; N, 6.33, 6.08. ^{1}H NMR (acetonitrile-d_3): Ph, 7.5−7.7 ppm (m); N(CH_3)$_2$, 2.57, 2.67 (t, $^3J_{PH}$ = 10.1 Hz); PCH_2CH_2P, 2.3−3.0 ppm (m); PCH_2CH$_3$, 1.98 ppm (dq, $^3J_{HH}$ = 7.7 Hz, $^2J_{PH}$ = 2.1 Hz); PCH$_2$CH_3, 1.16 ppm (dt, $^3J_{PH}$ = 17.0 Hz).

Acknowledgment. The support of the U.S. Department of Energy, Basic Energy Sciences Division, Office of Energy Research, and the U.S. Department of Energy Biofuels Systems Division as part of the Biofuels Program is gratefully acknowledged.

IC941144F